Planetary and Space Science 118 (2015) 256–266

Contents lists available at ScienceDirect

Planetary and Space Science

journal homepage: www.elsevier.com/locate/pss

# Against the biases in spins and shapes of asteroids

A. Marciniak [a,*], F. Pilcher [b], D. Oszkiewicz [a], T. Santana-Ros [a], S. Urakawa [c], S. Fauvaud [d,e], P. Kankiewicz [f], Ł. Tychoniec [a], M. Fauvaud [d,e], R. Hirsch [a], J. Horbowicz [a], K. Kamiński [a], I. Konstanciak [a], E. Kosturkiewicz [g,h], M. Murawiecka [a], J. Nadolny [a,i], K. Nishiyama [c], S. Okumura [c], M. Polińska [a], F. Richard [e], T. Sakamoto [c], K. Sobkowiak [a], G. Stachowski [g], P. Trela [a]

[a] Astronomical Observatory Institute, Faculty of Physics, A. Mickiewicz University, Słoneczna 36, 60-286 Poznań, Poland
[b] 4438 Organ Mesa Loop, Las Cruces, NM 88011, USA
[c] Bisei Spaceguard Center, Japan Spaceguard Association, 1716-3, Okura, Bisei, Ibara, Okayama 714-1411, Japan
[d] Observatoíre du Bois de Bardon, 16110 Taponnat, France
[e] Association T60, 14 avenue Edouard Belin, 31400 Toulouse, France
[f] Astrophysics Division, Institute of Physics, Jan Kochanowski University, Świetokrzyska 15, 25-406 Kielce, Poland
[g] Mt. Suhora Observatory, Pedagogical University, Podchorążych 2, 30-084 Cracow, Poland
[h] Astronomical Observatory of the Jagiellonian University, Orla 171, 30-244 Cracow, Poland
[i] Universidad de La Laguna, Department Astrofisica, E.38206 La Laguna, Tenerife, Spain

ARTICLE INFO

*Article history:*
Received 1 March 2015
Received in revised form
20 May 2015
Accepted 2 June 2015
Available online 12 June 2015

*Keywords:*
Asteroids
Lightcurves
Selection effects

ABSTRACT

Physical studies of asteroids depend on an availability of lightcurve data. Targets that are easy to observe and analyse naturally have more data available, so their synodic periods are confirmed from multiple sources. Also, thanks to availability of data from a number of apparitions, their spin and shape models can often be obtained, with a precise value of sidereal period and spin axis coordinates.

Almost half of bright ($H \leq 11$ mag) main-belt asteroid population with known lightcurve parameters have rotation periods considered long ($P \geq 12$ h) and are rarely chosen for photometric observations. There is a similar selection effect against asteroids with low lightcurve amplitudes ($a_{max} \leq 0.25$ mag). As a result such targets, though numerous in this brightness range, are underrepresented in the sample of spin and shape modelled asteroids. In the range of fainter targets such effects are stronger. These selection effects can influence what is now known about asteroid spin vs. size distribution, on asteroid internal structure and densities and on spatial orientation of asteroid spin axes.

To reduce both biases at the same time, we started a photometric survey of a substantial sample of those bright main-belt asteroids that displayed both features: periods longer than 12 h, and amplitudes that did not exceed 0.25 magnitude. First we aim at finding synodic periods of rotation, and after a few observed apparitions, obtaining spin and shape models of the studied targets.

As an initial result of our survey we found that a quarter of the studied sample (8 out of 34 targets) have rotation periods different from those widely accepted. We publish here these newly found period values with the lightcurves.

The size/frequency plot might in reality look different in the long-period range. Further studies of asteroid spins, shapes, and structure should take into account serious biases that are present in the parameters available today. Photometric studies should concentrate on such difficult targets to remove the biases and to complete the sample.



## 1. Introduction

Spin and shape parameters of a large sample of main belt asteroids are an important basis for theories describing Solar System formation and evolution, with non-gravitational forces influencing the orbital and physical properties of these minor bodies. It has been recently found that asteroids belonging to the Flora family have preferential prograde rotation, because retrograde rotating objects were moved by the Yarkovsky effect to the $\nu_6$ resonance at the inner main belt and removed (Kryszczyńska, 2013). This fact finds its confirmation in preferential retrograde rotation of Near Earth Asteroids (La Spina et al., 2004). It has also

* Corresponding author. Tel.: +48 61 8292780; fax +48 61 8292772.
*E-mail address:* am@amu.edu.pl (A. Marciniak).

http://dx.doi.org/10.1016/j.pss.2015.06.002
0032-0633/

been found that the distribution of known spin axis positions of small asteroids shows a trend for them to group at extreme values of obliquities (at high angles from their orbital planes), which can be explained as the outcome of spin evolution under the influence of YORP effect (Hanuš et al., 2013).

However, the available sample of well studied asteroids is burdened with substantial selection effects. There exist well known strong observational biases against small, low-albedo, and distant objects due to limitations of instruments that are most widely used for photometric studies. But there are also other strong selection effects that are connected to photometric studies.

The arithmetic mean of periods in the size range limited by absolute magnitude $H \leq 11$ mag given by Pravec and Harris (2000) was around 9–10 h, with a most extreme value of the mean equal to 12 h in the size range around 100 km. With time the sample of asteroids with known periods substantially grew, and a large number of slow periods was found. Currently the arithmetic mean of rotation periods in this size range is almost 20 h. Median value of all known periods in this sample of main-belt objects with $H \leq 11$ mag (where the period survey is almost complete) is around 11 h. It means that half of the bright main-belt population with known lightcurve parameters have rotation periods considered "long" and are rarely chosen as targets for photometric observations, even though they are easy targets for small telescopes. As a result only 20% of this group has been spin and shape modelled. Along with the bias against asteroids with long periods of rotation (here: $P \geq 12$ h), there is another one, against those with low lightcurve amplitudes (here: $a_{max} \leq 0.25$ mag). Within the set of bright asteroids those with small amplitudes comprise almost half of the whole studied population, while spin and shape models have been determined for around 20% of this sub-population (source: LCDB; Warner et al., 2009, see Table 1). On the other hand two remaining populations (short-period, and high-amplitude objects) have been modelled in 36% each (see Fig. 1). By chance, at such conditions statistics in both groups, divided by period and by maximum amplitude, are very similar and both diagrams look almost identical to each other. For fainter targets these inequalities are much stronger, and the data pool of objects with known periods is highly incomplete. Moreover, the widely known plot showing distribution of rotational frequency vs. asteroid sizes might in reality look slightly different in the lower-right part (Fig. 2).

In the sample of main-belters with $H \leq 11$ mag and with available lightcurves, only 13% of long-period objects with low amplitudes have been spin and shape modelled, while 43% of the comparably numerous group with opposite features (periods shorter than 12 h and maximum amplitudes higher than 0.25 mag) have been modelled (see Table 2 and Fig. 3). It means that almost half of the easily observable population is well studied, while objects more difficult to properly observe and analyse are well studied in a much smaller fraction of their population.

The observational bias against asteroids with small amplitude of brightness variations can influence our knowledge of the asteroid spin axis distribution in space, on their shapes and densities. Since weakly elongated objects always display small lightcurve amplitudes, their periods are hard to determine, and their spin and shape models are very hard to obtain. They become even more difficult for modelling when their spin axes are close to their orbital planes, causing any brightness variations disappear when asteroid is viewed nearly pole-on (Marciniak and Michałowski, 2010). Moreover, data for low-amplitude objects can be lost in the 0.1–0.2 magnitude noise of the sparse data coming from large, astrometric surveys (Hanuš et al., 2011), making them hard to be modelled using such data alone. Photometric data for unique spin and shape modelling of low-amplitude asteroids should be at least an order of magnitude better, with the noise not exceeding 0.01 mag.

Small, kilometer sized asteroids with long periods of rotation can be those that have been spun down by YORP torques (Rubincam, 2000) or can be in tumbling rotational states, showing double periodicity. Thus they are important targets for studies of damping timescales and evolution under thermal effects. Additionally, studies in the small amplitude range can result in possible discoveries of binary systems, because in majority of binaries the components are weakly elongated in shape (Pravec and Harris, 2007).

Summing up, it turns out that at least half of the whole well observable main belt population is studied insufficiently, and the selection effects tend to increase with time. Previously found groupings and depopulations within large number of asteroid spin axis longitudes could have been caused by several overlapping selection effects (Bowell et al., 2014). Also, it has been shown that even precise data from the Gaia satellite will introduce biases in derived asteroid spin and shape models depending on their true pole latitude and shape elongation (Santana-Ros et al., 2015).

## 2. Observing campaign

Motivated by these facts we started a large, long-term observing campaign of a substantial sample of long-period asteroids from those objects (highlighted with rectangular frame in Fig. 2) that additionally displayed small amplitudes of brightness variations, to reduce both selection effects at the same time. Our aim is to obtain spin and shape models of this class of "difficult" objects in order to reduce the increasing biases favouring quickly rotating, elongated asteroids, with extreme values of spin axis obliquity to be prevailingly observed and modelled today. It is caused by the fact that the latter objects are easiest to observe and analyse – their short periods allow for a full lightcurve coverage in one or two nights, and large amplitudes make their brightness variations always stand out of the noise even in imperfect observing conditions. On the other hand, obtaining full phase coverage for objects with long periods requires much more telescope time and, if their amplitude is small, data of higher quality. The periods of the order of several dozens of hours have to be determined from fragments

**Table 1**
Numbers of asteroids with $H \leq 11$ mag, for which LCDB (Warner et al., 2009) gives physical parameters. Only lightcurve parameters with period quality code better than or equal to 2− have been included. The total number here is 1230 asteroids, median period is 10.986 h, median $a_{max} = 0.27$ mag. Parentheses give numbers of spin and shape modelled objects within each group.

| Period of rotation | | | Maximum amplitude | | |
|---|---|---|---|---|---|
| Long, $P \geq 12$ h (modelled) | short, $P < 12$ h (modelled) | Undefined | High, $a_{max} > 0.25$ mag (modelled) | Low, $a_{max} \leq 0.25$ mag (modelled) | Undefined |
| 528 (101) | 656 (236) | 46 | 655 (233) | 543 (104) | 32 |

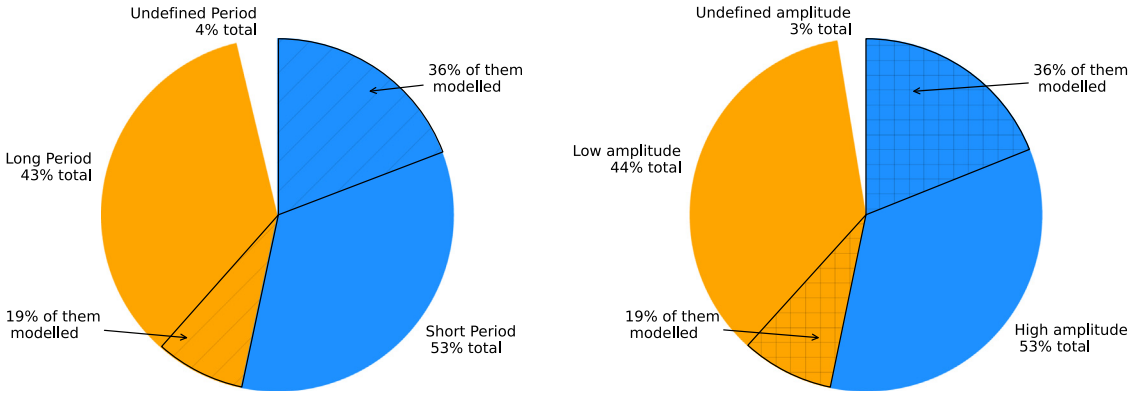


**Fig. 1.** Statistics of periods and amplitudes of bright main-belt asteroids, based on data from Table 1.

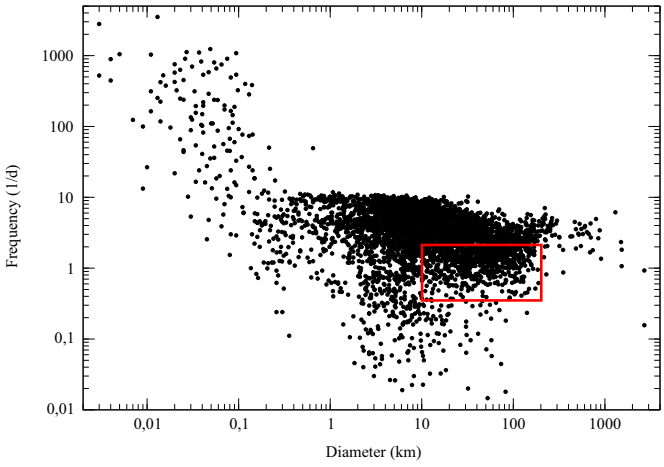


**Fig. 2.** A diagram of asteroid rotational frequencies versus sizes (after Warner et al., 2009). Rectangular frame highlights class of objects studied within this project.

covering only a small fraction of a full rotation. If the lightcurves are symmetric – i.e. both maxima look similar – making a composite lightcurve can often lead to finding an alias period like 2/3 or 3/2 of the true period. This might be a potential source of another bias: asteroids with long periods, even if well observed, can have their periods determined incorrectly. This effect can be even stronger for objects displaying both features – long period and low amplitude – at the same time.

We restricted our statistical studies of present state to the sample of main-belt asteroid brighter than 11 absolute magnitude, because in this group the survey of lightcurve parameters is almost complete. This set roughly coincides with the first thousand of

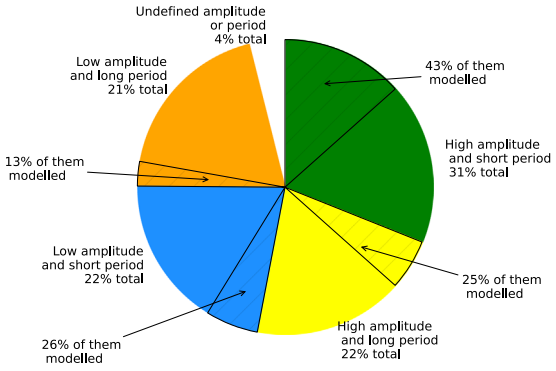


**Fig. 3.** Statistics of periods and amplitudes of bright main-belt asteroids based on two parameters simultaneously, based on data from Table 2

**Table 2**
Same as Table 1 but for two parameters simultaneously. Parentheses give numbers of spin and shape modelled objects within each group.

| High amplitude and short period | High amplitude and long period | Low amplitude and short period | Low amplitude and long period | Undefined amplitude or period |
|---|---|---|---|---|
| 382 (165) | 270 (68) | 272 (71) | 258 (33) | 48 |

numbered asteroids. Also, it has been shown that all main-belt objects have been discovered down to the absolute magnitude 11.25 (Jedicke and Metcalfe, 1998). A great majority of these asteroids are objects with bright apparent magnitude (not fainter than 14 mag), well within reach of small amateur telescopes. Still, many of them are insufficiently studied, not even allowing for a unique period determination. There is a clear correlation between the number of apparitions in which an asteroid has been observed and its period. When the period is known to be longer than 10–12 h it is avoided by most observers. It is understandable, because the telescope time is often very limited, and such objects often cannot be observed over full rotation from one site for example due to certain commensurabilities with Earth day.

As for the bias against small amplitudes, the limitations here are of a different nature. Quite often lightcurve amplitudes of such objects are at the level of a few hundredths of a magnitude. It requires good instrumental and weather conditions, so that the data are not burdened with noise greater than a few thousandths of a magnitude. Since small telescopes and very short exposure times are most widely used, this level of precision cannot always be reached. Sometimes the data can be binned to decrease the noise – an efficient strategy for objects with long periods. It is also possible that seemingly flat lightcurves were considered uninteresting and left unpublished, while simple rescaling of the plot (stretching the magnitude scale and compressing the time scale) would show them to be clear fragments of a long-periodic lightcurve, where adding a few more such fragments would suffice for completion. We encourage observers to submit such data to ALCDEF repository,[1] even if incomplete, they can be very useful for asteroid modelling.

Our target selection procedure was as follows: all the long-period ($P \geq 12$ h) and low-amplitude ($a_{max} \leq 0.25$ mag, or 0.35 mag in single cases) asteroids without spin and shape models were included from the list of main belt asteroids with absolute magnitude brighter or equal to 11 mag, with the exception of

[1] http://www.minorplanet.info/alcdef.html

**Table 3**
Observatories participating in this project, with their abbreviated names, IAU codes, coordinates, and telescope diameters.

| Observatory name | Abbreviated name | IAU code | Location | Telescope diameter (m) |
|---|---|---|---|---|
| Borowiec Observatory (Poland) | Bor. | 187 | 52°N, 17°E | 0.4 |
| Montsec Observatory (Catalonia, Spain) | OAdM | C65 | 42°N, 01°E | 0.8 |
| Organ Mesa Observatory (NM, USA) | Organ M. | G50 | 32°N, 107°W | 0.35 |
| Winer Observatory (AZ, USA) | Winer | 648 | 32°N, 111°W | 0.70 |
| Bisei Spaceguard Center (Okayama, Japan) | Bisei | 300 | 35°N, 134°E | 0.5 and 1 |
| JKU Astronomical Observatory (Kielce, Poland) | Kie. | B02 | 51°N, 21°E | 0.35 |
| Mt. Suhora Astronomical Observatory (Poland) | Suhora | – | 50°N, 20°E | 0.25 and 0.60 |
| Pic du Midi Observatory (France) | Pic | 586 | 43°N, 0°E | 0.6 |

objects belonging to certain groups and families that are studied by other researchers to avoid duplication, and single cases of very long period objects ($P > 50$ h), for practical reasons. Asteroids with periods longer than 50 h present only 3% of the studied population. While they deserve to be studied for many reasons like a possibility of tumbling rotational state or a binarity, a separate large observing campaign would be needed for them. Still, since they comprise only a small part of the studied population, we do not introduce a large bias by omitting them. On the other hand we included objects with unknown or uncertain period, because that most probably means "long". The bias that we conserve here is the one against faint targets, because of the equipment limitations. But with an access to larger telescopes, we are going to address this bias as well, extending our target list to fainter objects, where the selection effects studied here are even more profound. As of now our target selection resulted in the list of 120 bright main-belt asteroids (almost half of the population of long-period and low-amplitude objects within this brightness range) and up till December 2014 we gathered data for 45 of them (see the Results section).

For the needs of this project we set up an international network of observatories, with the local observing station at the Borowiec Station of Poznań Astronomical Observatory Institute (Poland) being the main site. Other observatories are Observatori Astronòmic del Montsec – OAdM – in Catalonia (Spain); Organ Mesa Observatory in New Mexico (USA); Winer Observatory in Arizona (USA); Bisei Spaceguard Center (Japan)[2]. We also get an occasional support from Jan Kochanowski University in Kielce and Mnt. Suhora observatories (Poland), and Observatoire du Pic du Midi (France). Their locations and telescope parameters are summarised in Table 3. Such network allows for effective coordination of the observing campaign, for example for asteroids with periods close to 12 or 16 h, or their integer multiples. The crop of the observing campaign conducted over last two years consists of 1670 h of data.

Because of the small amplitudes of lightcurves, good quality photometry is necessary, with the noise at the level of a few tenths of a percent. Such quality data are being regularly obtained in the Borowiec Station of Poznan Astronomical Observatory Institute. During more than fifteen years of station operation optimal observing and reduction procedures have been established and substantial experience has been gained both in asteroid photometry and modelling (see Michałowski et al., 2004 for the description of the station and reduction procedures, and e.g. Marciniak et al., 2012 for lightcurves and models).

We perform photometric observations of asteroids using Red and Clear filters, with standard bias, dark frame, and flatfield corrections. At the next stage the aperture photometry is applied with a high level of automatisation, but with a careful control of a comparison star colours and possible intrinsic variability; a cross check between at least three different comparison stars is performed to exclude it. Also, any field star passages and possible interfering artifacts, like satellite trails and seeing changes, are checked, together with other possible instrumental problems. A resulting fragment of a relative lightcurve is binned when necessary, so that the number of datapoints per period would not exceed 200.

It might seem that in case of long-period objects performing an absolute photometric measurements is the right choice. However we rely on relative rather than absolute photometric measurements, for the following reasons. First of all the observing conditions in our local observing station are rarely photometric, making measurements of absolute magnitudes burdened with serious errors. But the main reason is that we are in the small amplitude range, with amplitudes of some objects being below 0.1 mag. Having the uncertainties of absolute magnitude measurements normally at the level of a few hundredths of a magnitude would lead to a situation where the measurement uncertainties are of the same order as the determined values (amplitudes). In the end an arbitrary shifting in the magnitude scale would be necessary, meaning that the absolutisation was done in vain.

Our observing campaign relies on optimised observing strategy and careful planning of possible phase coverage from multiple stations. We aim at obtaining at least one long lightcurve fragment and completing the whole rotation with shorter fragments, or of similar in length, when the observing circumstances allow. The data are reduced and composite lightcurves are made shortly after an observing session, so that new observations can be planned when an asteroid can still be reached. When a new period is found the campaign is intensified, focusing on this object to confirm the new value and exclude any possible alias periods. When the period is well known we are also trying to register the phase angle effects, e.g. growing amplitude, which requires observing at least 1/4 of the full rotation in a single session. However with periods exceeding 30 h, that is often impossible. For a precise period determinations we rely on the repeatable fragments of the lightcurves and realistic constraints put on the lightcurves with higher harmonics (Harris et al., 2014). Our group has access to the 80-cm robotic telescope in OAdM Observatory in the Montsec range on the south-west side of the Pyrenees. To increase the return of data gathering on such an instrument we are utilising the 100 h granted each year with the observing strategy of obtaining single images of each object at half hour intervals. It facilitates observing a greater number of long-period objects in a much shorter time compared to traditional continuous photometry, at the same time not altering the details of the resulting lightcurves, as we repeat such observations until we gather at least 100 points per period. The acquired know-how served in similar observations on another robotic telescope: the 0.7 m GATS-PST2 telescope built in our institute in Poland and recently moved to Winer Observatory in Arizona.

[2] Bisei Spaceguard Center is administrated by the Japan Space Forum.

## 3. Results

At this stage none of the asteroids observed in our programme has enough data for a unique spin and shape model. However, as an intermediate goal, we determined synodic periods for all the objects observed. To our own surprise we found periods differing from those previously accepted for as many as 8 out of 34 well observed asteroids (those for which the amount of data allows for a unique period determination; see Table 4). The quality codes for their periods in LCDB summary line were "2" (period certain within 30%, or to an integer ratio), but also "3" which means a secure period determination. From the remaining number of 11 studied objects at least 2 also show values of periods different from those in the LCDB, but the amount of data we gathered for them does not allow for making firm conclusions yet. We decided to publish here those newly found periods that we consider secure, together with composite lightcurves for these 8 asteroids. They are a significant fraction of the sample (24%) studied by us, confirming that this class of objects is burdened with serious bias in basic physical parameters in addition to the observing biases that prevent most of them from being studied according to the number in their population. Studied here objects make up around 1/5 of the whole population of bright main-belt asteroids. Since 1/4 of the sample that we studied showed to have different periods to those widely accepted, we can assume that at least 1/20 of the main-belt population probably still have their periods determined incorrectly (this would mean a few dozen objects from the first thousand of numbered asteroids). It applies even more to fainter objects, where the uncertainties are greater and where many do not have any period determinations.

In Fig. 4 we show the rotation frequencies versus diameters of the studied asteroids. One set comes from LCDB (Warner et al., 2009) and is marked with filled circles, and the other set presents our results (new periods with the same diameters) marked with diamonds. Both sets mostly coincide, but for 8 objects we see substantial shift in frequency scale, mostly downwards, to lower frequencies (longer periods). The scale is set to cover the rectangular area from Fig. 2.

Figs. 5–12 show the composite lightcurves of those asteroids for which we found new values of the period. These composites have been created using the procedure described by Magnusson and Lagerkvist (1990). The individual lightcurves have been

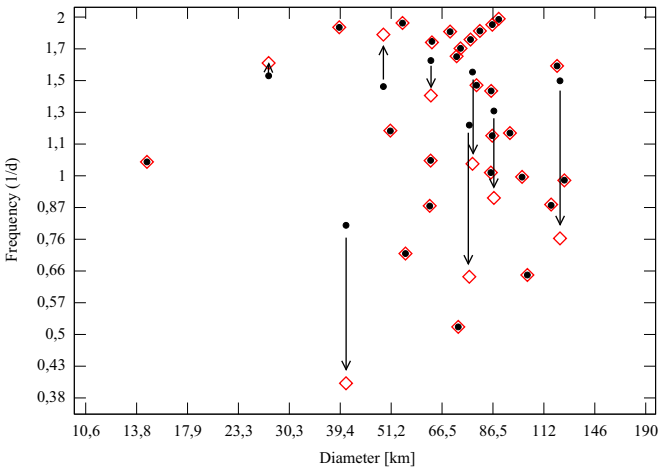


**Fig. 4.** Rotation rate (frequency) versus diameter of the objects studied. Filled circles denote data based on LCDB, diamonds denote frequencies found in this work, while diameters remain the same. The scale coincides with the rectangular frame from Fig. 2.

**Table 4**
Asteroid synodic periods and amplitudes found within this project compared to literature data gathered previously in LCDB (Warner et al., 2009) as for November 2012.

| Asteroid name | Diameter (LCDB) (km) | Amplitude (LCDB and *this work*) (mag) | Period (LCDB) (h) | U code | Period (this work) (h) |
|---|---|---|---|---|---|
| **(70) Panopaea** | 122.17 | 0.06 – *0.14* | **15.797** | 3 | **31.619** ± 0.007 |
| (159) Aemilia | 124.97 | 0.17 – *0.26* | 24.476 | 3– | 24.485 ± 0.002 |
| (172) Baucis | 62.43 | *0.21* – 0.35 | 27.417 | 3 | 27.402 ± 0.005 |
| (195) Eurykleia | 85.71 | 0.10 – 0.24 | 16.521 | 3 | 16.518 ± 0.002 |
| (202) Chryseis | 85.58 | 0.04 – *0.28* | 23.670 | 3 | 23.668 ± 0.002 |
| **(219) Thusnelda** | 40.56 | 0.19 – *0.24* | **29.842** | 3 | **59.74** ± 0.02 |
| **(227) Philosophia** | 86.90 | 0.06 – 0.20 | **18.048** | 2 | **26.46** ± 0.01 |
| (236) Honoria | 86.20 | 0.05 – *0.27* | 12.333 | 3 | 12.338 ± 0.002 |
| (301) Bavaria | 54.27 | 0.28 – *0.31* | 12.253 | 3 | 12.243 ± 0.002 |
| **(305) Gordonia** | 49.17 | 0.16 – *0.23* | **16.2** | 2 | **12.893** ± 0.002 |
| **(329) Svea** | 77.83 | 0.09 – 0.26 | **15.201** | 3 | **22.778** ± 0.006 |
| (335) Roberta | 89.10 | 0.05 – *0.19* | 12.054 | 3 | 12.027 ± 0.003 |
| (380) Fiducia | 73.19 | 0.04 – 0.32 | 13.69 | 3 | 13.70 ± 0.02 |
| (387) Aquitania | 100.51 | *0.18* – 0.25 | 24.144 | 3 | 24.13 ± 0.01 |
| (395) Delia | 50.98 | *0.16* – 0.25 | 19.71 | 2 | 19.680 ± 0.005 |
| **(439) Ohio** | 76.57 | *0.23* – 0.24 | **19.2** | 2, A | **37.46** ± 0.01 |
| (476) Hedwig | 116.76 | 0.13 – *0.17* | 27.33 | 3 | 27.246 ± 0.005 |
| (478) Tergeste | 79.46 | *0.15* – *0.30* | 16.104 | 2+ | 16.105 ± 0.001 |
| (483) Seppina | 69.37 | 0.14 – 0.29 | 12.727 | 3 | 12.719 ± 0.002 |
| (487) Venetia | 63.15 | 0.03 – 0.30 | 13.28 | 2 | 13.342 ± 0.002 |
| (501) Urhixidur | 77.06 | *0.12* – 0.14 | 13.1743 | 3 | 13.175 ± 0.002 |
| (524) Fidelio | 71.73 | 0.18 – 0.22 | 14.198 | 3 | 14.177 ± 0.005 |
| (538) Friederike | 72.34 | 0.03 – 0.25 | 46.728 | 3 | 46.7 ± 0.3 |
| (618) Elfriede | 120.37 | 0.12 – 0.20 | 14.801 | 2 | 14.800 ± 0.005 |
| (653) Berenike | 39.18 | 0.03 – 0.11 | 12.4886 | 3 | 12.481 ± 0.006 |
| **(666) Desdemona** | 27.22 | 0.11 – *0.22* | **15.45** | 2 | **14.607** ± 0.004 |
| (667) Denise | 80.85 | 0.24 – *0.25* | 12.687 | 3 | 12.686 ± 0.003 |
| (672) Astarte | 14.54 | 0.10 – *0.17* | 22.572 | 3 | 22.588 ± 0.005 |
| (780) Armenia | 94.40 | 0.10 – 0.18 | 19.891 | 3 | 19.89 ± 0.01 |
| (788) Hohensteina | 103.29 | 0.12 – 0.18 | 37.176 | 3 | 37.13 ± 0.05 |
| **(806) Gyldenia** | 62.82 | 0.10 – 0.27 | **14.45** | 2 | **16.852** ± 0.006 |
| (907) Rhoda | 62.73 | *0.08* – 0.16 | 22.44 | 3– | 22.45 ± 0.01 |
| (980) Anacostia | 86.19 | *0.05* – *0.18* | 20.117 | 3 | 20.113 ± 0.004 |
| (1062) Ljuba | 55.10 | *0.11* – 0.17 | 33.8 | 3 | 33.79 ± 0.02 |

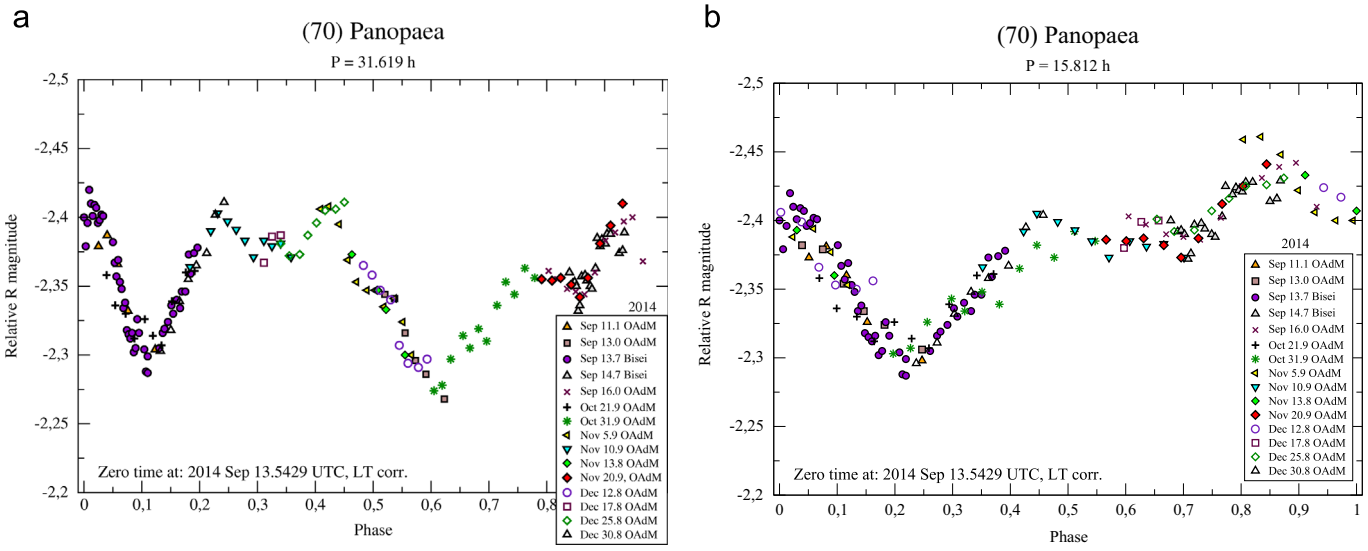


**Fig. 5.** Composite lightcurve of (70) Panopaea in the year 2014, with the best-fit period on the left and half period on the right.

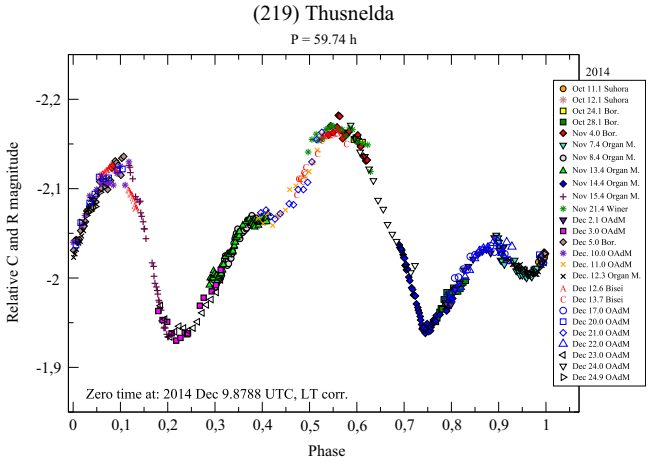


**Fig. 6.** Composite lightcurve of (219) Thusnelda in the year 2014.

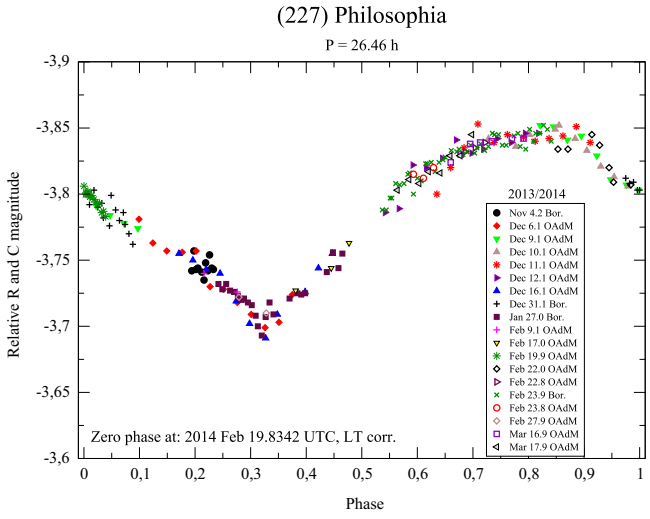


**Fig. 7.** Composite lightcurve of (227) Philosophia in the years 2013/2014.

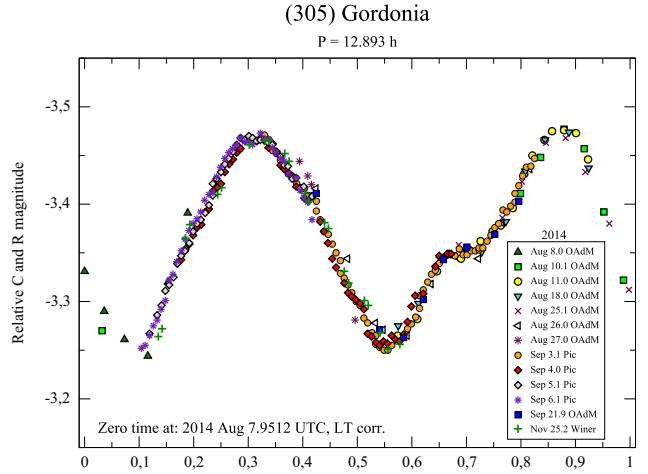


**Fig. 8.** Composite lightcurve of (305) Gordonia in the year 2014.

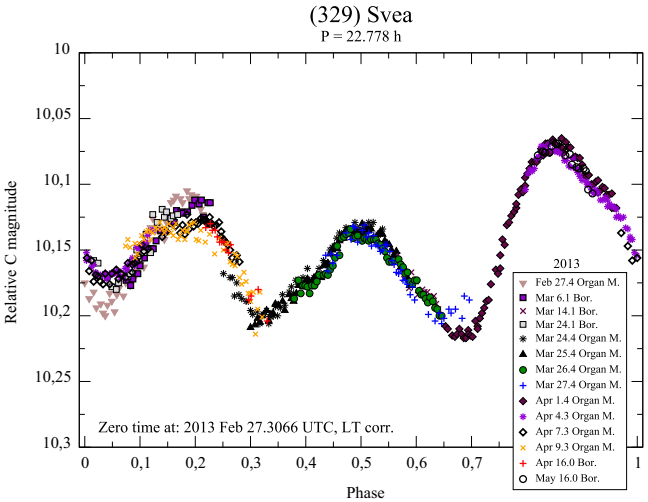


**Fig. 9.** Composite lightcurve of (329) Svea in the year 2013.

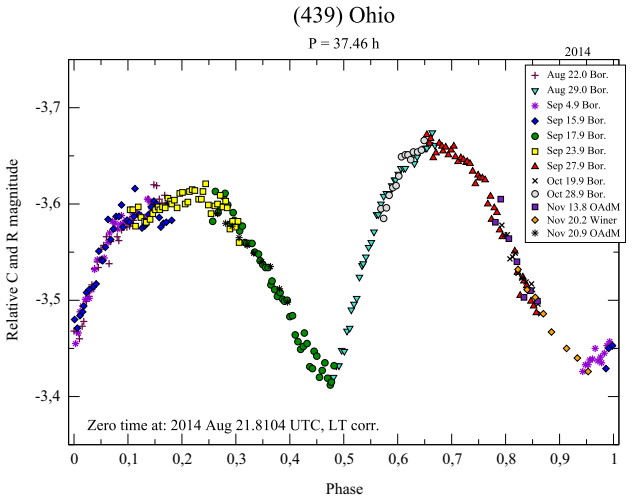


**Fig. 10.** Composite lightcurve of (439) Ohio in the year 2014.

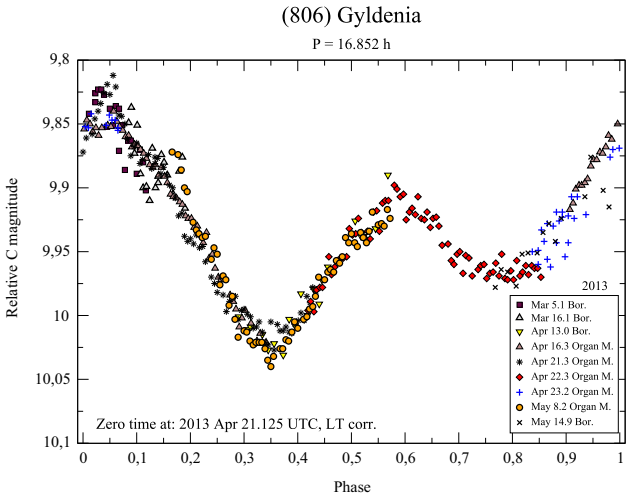


**Fig. 12.** Composite lightcurve of (806) Gyldenia in the year 2013.

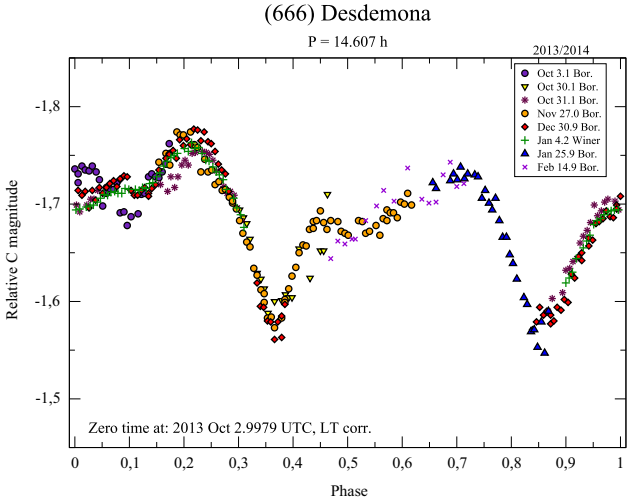


**Fig. 11.** Composite lightcurve of (666) Desdemona in the years 2013/2014.

composited with the best fitting synodic period written in the graphs. Points from different nights are marked with different symbols. The vertical position of each individual lightcurve is obtained to minimise the dispersion of data points relative to their neighbours. The abscissae are the rotational phases with the zero points corrected for light–time. After the best value for the period was found, the composite lightcurves were tried with various values of the period close to the best one (in terms of $\chi^2$). Those giving almost equally good fits of the fragments to each other were accepted, until notably worse fit was found. This way the range of good periods was established and half of its value was accepted as the period uncertainty.

In addition to best fit-lightcurves we present period spectra for each of these targets (see Figs. A1–A8 in the Appendix). In all cases period found here gives substantially lower RMS value than previously accepted one. However in one case the period accepted here cannot be distinguished from its double. See the discussion for (227) Philosophia in Section 3.3 for the best period selection criteria.

The following subsections describe in detail previous works and our findings concerning specific objects. Lightcurves of the remaining objects of the studied sample will be published when enough data are gathered to facilitate obtaining their spin and shape models. However the synodic periods that we found for them agree with the values accepted in LCDB within 1% or less (see Table 4).

Table 4 presents our main results. After asteroid numbers and names, it gives their diameters cited after LCDB. The third column contains amplitude range ($a_{min}$ and $a_{max}$) from LCDB updated with the values found within this survey, marked with italics. The last two columns present periods of rotation: the one from the LCDB summary line, and the period found in this study with uncertainty values. We mark with boldface those targets for which periods found here differ substantially from the previously accepted values. In the table we cite the period values as they were in the summary line of the November 2012 public release of the LCDB, when we were starting our project. In the meantime, three values of the LCDB periods have changed. They are cited in respective subsections.

### 3.1. (70) Panopaea

Previous observations of Panopaea were conducted by Schroll and Schober (1983), and Harris and Young (1989) in the year 1980. Both resulted in slightly asymmetric, bimodal lightcurves of 0.12–0.11 mag amplitude that were composited on a basis of 15.87 and 15.797 h period, respectively. Next, Panopaea was observed by Denchev et al. (1998) who only recorded an amplitude greater than 0.1 mag, and by Behrend et al. (2014) in 2006, when it displayed a lightcurve where one of the maxima in the 15.79-h composite was almost gone, and an amplitude was as small as 0.06 mag.

We observed (70) Panopaea from early September till late December 2014. We noticed that 15.812 h composite lightcurve (best fitting in this period range) gave noticeable worse fit than its double: 31.619 h (see Fig. 5). For example the fragments from 13.7 September (filled circles), 13.0 September (filled squares), and 31.9 October (stars) have different slopes, although obtained close in time. These fragments suggest the presence of two minima: one narrow, and the other wider. We are aware that the phase angle effects might slightly change the character of the lightcurve, but we consider the apparent misfits too big for those effects acting over a few weeks. We conclude that the period of this asteroid is 31.619 h rather than 15.812, but it needs further confirmation in the next apparitions. The light variations amplitude in the year 2014 was 0.14 mag ($\pm$0.02 mag), a small value, but the biggest observed for Panopaea so far.

### 3.2. (219) Thusnelda

This bright, main-belt asteroid was observed in the year 1981, by Lagerkvist and Kamel (1982), and by Harris et al. (1992). No other lightcurve has been obtained since then. Both groups determined a rotation period around 29.8 h (29.76 h and 29.842 h, respectively) from around 7 lightcurve fragments. The amplitude was at the level of 0.20–0.19 mag and the composite lightcurves showed one maximum with a "shelf" before it, which could be considered a second maximum.

We observed Thusnelda in the year 2013 apparition, but the results were inconclusive in terms of the period, because of too short lightcurve fragments. However, in 2014 we obtained a wealth of data, which clearly indicate the period of 59.80 h, which is close to double the value previously accepted (see Fig. 6). The amplitude is $0.24 \pm 0.01$ mag. The composite lightcurve shows interesting features with a shelf before one of two maxima, and a bump in one of the minima. We covered almost each phase multiple times to confirm the new period, but it took no more than 10 longer fragments to determine its value. Data from previous apparitions fit the new period well. Almost 60-hour period, although very long, turned out not that difficult to be found and fully covered, even though only relative lightcurves were used. This fact is encouraging for further works on long-period asteroids. When in the low-amplitude range, they tend to display irregular lightcurve features that help us to resolve the period.

### 3.3. (227) Philosophia

Philosophia was observed multiple times by various authors, but the correct value of its rotation period is still ambiguous. Bembrick et al. (2006), basing on observations from 2004 and 2005 determined period of 18.048 h, Behrend et al. (2014) in 2006 apparition, found the period of 26.138 h. Alkema (2013a) observed Philosophia in 2012 and found the period of 17.181 h. Lastly, Pilcher and Alkema (2014a,b) observed this asteroid in 2013/2014 apparition and published the period of 52.98 h, but later revised it to an ambiguity between 26.476 h and 52.955 h. At the beginning of our project the value accepted in the LCDB for the period of Philosophia was 18.048 h with the code "2"; now it is 52.98 h with the code "2" and a flag "A" (ambiguous). The amplitudes of the previously recorded lightcurves ranged from 0.06 to 0.20 mag, with one determination at 0.35 mag by Ditteon and Hawkins (2007) in 2006, which is probably erroneous. The lightcurves of low amplitude were very irregular, but those of larger ones were more symmetric.

It is worth noting that in 2006 a seemingly bimodal 26.138-h period lightcurve with two clear minima was recorded (Behrend et al., 2014). However the data for the two minima are spaced by tens of days, thus a large number of rotations (39.5), and actually can cover the same minimum, if the period had a slightly different value (26.46 h proposed in this work), then these minima would be spaced by exactly 39.0 cycles.

In this work we observed Philosophia independently from November 2013 till March 2014 mostly using the 80-cm TJO robotic telescope in the Montsec Observatory (OAdM). Basing on 19 nights of data we found the most probable period of 26.46 h in a 0.15 mag ($\pm 0.02$ mag) amplitude lightcurve of a monomodal character (Fig. 7) confirming the values published by Behrend et al. (2014) and Pilcher and Alkema (2014b). Our lightcurve contained small irregularities that would repeat themselves in the second half of the lightcurve if the period was forced to the double value 52.92 h. Our data from 2013/2014 apparition folded with the data by Pilcher and Alkema (2014a) from similar time confirm the fact that bimodal, 53-h composite lightcurve would be conspicuously symmetric over half rotation, implying the same shape irregularities at both sides of the body. We consider the 26 h period the most probable also because it probably implies a switch from bimodal to monomodal lightcurve character between the years 2006 and 2013/2014, a behaviour seen before in many asteroids with strongly inclined spin axes. Such switch is caused by changing viewing geometry. When the asteroid is viewed near an equatorial aspect it usually displays roughly regular, bimodal lightcurve, while viewed nearly pole-on, the asteroid displays lightcurve that is almost flat or changes its character to monomodal or more complicated, but always of a small amplitude. In case of Philosophia, also a change in the angular distance from the ecliptic plane could play a role in the changes of the lightcurve, being maximal in the year 2006 and minimal in 2013/2014. The 26-h period was already shown to fit also the data from 2012 (Pilcher and Alkema, 2014b).

### 3.4. (305) Gordonia

Gordonia was observed by Lazar et al. (2001) in the year 2000, Menke et al. (2008) in 2005, and Behrend et al. (2014) in 2008, and as a result three values were published for the rotation period: 16.2, 12.89, and over 10 h, respectively. In 2005, when the only full lightcurve was obtained, Gordonia showed a bimodal lightcurve with wide maxima and some visible phase angle effects or some instrumental artifacts. Registered amplitudes ranged from around 0.1 to 0.17 mag, though it seems that the higher value should be 0.27 mag, based on data from 2005 (Menke et al., 2008). We observed Gordonia in its apparition in summer 2014 and quickly realised that its period must be close to 12.89 h found by Menke et al. (2008). The large lightcurve fragments that we obtained phased with this period showed a clear, bimodal lightcurve with a small "shelf" before one of the maxima, and an amplitude of $0.23 \pm 0.02$ mag (Fig. 8). The final period after 3.5 months of observation was determined to be 12.893 h. The 16.2 and 10-h periods are ruled out on the basis of new data.

### 3.5. (329) Svea

Previous lightcurves of (329) Svea were published by Weidenschilling et al. (1990), Pray (2006), Behrend et al. (2014), and Menke et al. (2008). The first two authors give the rotation periods of 15.0 and 15.201 h and the remaining two 22.770 and 22.6 h, respectively. The lightcurves of 15-h periods had both a bimodal character. The lightcurves of 22-h period gave trimodal lightcurve in the year 2005 (Menke et al., 2008), but bimodal one in 2006 (Behrend et al., 2014). The highest quality code "3" in LCDB for the period determination was given to 15.201 h determined by Pray (2006), and that value was in the LCDB summary line in late 2012 when our target list was created (LCDB; Warner et al., 2009). Later, this value was changed to 22.77 h determined by Behrend et al. (2014), with the quality code "2+". It is worth to note that longer, 22-h periods, were determined on richer datasets than shorter, 15-h ones. However, some of the previously gathered data, namely those published by Menke et al. (2008), and Pray (2006), are rather noisy or consist of short fragments, so that many different periods are possible.

Our data from the apparition in March 2013 seemed to confirm 15 h period at first. However, in early April 2013 a maximum of much higher amplitude than previous two was observed. The composite lightcurve now could only be created with 3/2 of the previous period (namely with 22.778 h), producing three different maxima per full cycle, slightly changing their shape with phase angle (Fig. 9). The bimodal lightcurve of 15 h is not possible now, as can be inferred from the periodogram (Fig. A5). The new, longer period seems to depend on a single night of 1 April, but even without this night a much better fit is obtained for 22 h, than for 15 h period.

This way we confirmed the values given by Behrend et al. (2014) and Menke et al. (2008). The phase angle effects are especially visible in the shape and height of the first maximum in Fig. 9. First, in February 2013, two months before the opposition date, this maximum

was higher and peaked, then in March a notch on the top started to mark itself to become more evident in April, when the amplitude was smallest, as expected near the opposition. Such effects are not so profound in the remaining part of the lightcurve, because those fragments were obtained with much less time span between separate fragments. The amplitude in 2013 was $0.16 \pm 0.02$ mag, and the composite lightcurve was created on 14 fragments most of which covered 0.2–0.3 of the full cycle. The behaviour of this target apparently changes from simple bi-modal to tri-modal depending on an aspect, indicating an interesting shape and an inclined spin axis.

### 3.6. (439) Ohio

Observed previously in the year 1984 by Lagerkvist et al. (1987), asteroid Ohio displayed one wide maximum and a flat minimum in a 19.2 h lightcurve, with an amplitude of 0.24 mag. There are also data gathered by group led by Behrend et al. (2014) in 2004 and 2007 but these lightcurves were highly incomplete. A possibility of a bimodal lightcurve behaviour was mentioned by the first authors, if the period was twice as long, namely 38.4 h.

We confirmed that supposition, observing this target from August till November 2014. We found the best fit period an hour shorter than suggested by Lagerkvist et al. (1987), at 37.46 h, in a bimodal, slightly asymmetric lightcurve of $0.23 \pm 0.02$ mag amplitude (Fig. 10). The short period, 19.2 h, can be safely rejected based on new data.

### 3.7. (666) Desdemona

Desdemona was previously observed in three apparitions: in the year 2000 (Stephens, 2001), and in 2004 and 2006/2006 (Behrend et al., 2014). Here too, only the first publication contains full phase coverage, the period was determined at 15.45 h, and an amplitude at 0.11 mag. Data from next two apparitions suggested 9.2-h period and amplitudes ranging from 0.07 to 0.16 mag.

We observed Desdemona from October 2013 till February 2014, and had problems finding its period at first. Previously published values did not fit the new data, and the relatively good fit could only be obtained on the basis of 14.607 h, if some discrepancies could be assigned to phase angle effect (see Fig. 11). This is possible, since most overlapping fragments differ in time by a month or more. The composite lightcurve of this target contains two narrow minima and very wide, wavy maxima, and has an amplitude of $0.22 \pm 0.02$ mag.

### 3.8. (806) Gyldenia

Previously gathered lightcurves of this target come from the years 2005, 2007 (Behrend et al., 2014), and 2013 Alkema (2013b). Data from both 2005 and 2007 suggest a period of 14.45 h, but have incomplete coverage, and probably some observing artifacts in a form of sudden dimming at the end of the observing sessions. Apart from it, the amplitudes were 0.27 and 0.10 mag, respectively. Data published by Alkema (2013b) fit a different period: 16.846 h, and have a multiple phase coverage in a lightcurve of 0.14 mag amplitude. The new data were shown to misfit the period of 14.52 h. In the summary line in LCDB database the old value of period was changed to the new one, with a code $3-$.

We observed Gyldenia independently in 2013, and also found the old period value to be wrong. We found 16.856 h to fit best, which is a similar value to that published by Alkema (2013b). However, the amplitude of our lightcurve is substantially larger: $0.20 \pm 0.02$ mag (Fig. 12), though it was determined in the same apparition. There are two fragments in our composite lightcurve that stretch from peak to peak, and they were obtained under small phase angles (2° and 3°), so their amplitudes were not enlarged by phase angle effects. We suppose that the lower amplitude determined by Alkema (2013b) was caused by short fragments that could be arbitrarily shifted in vertical scale which suppressed the amplitude. The overall look of our composite lightcurve is highly asymmetric, with maxima and minima at notably different levels.

## 4. Conclusions and future work

We came across substantial selection effects among bright main-belt asteroids and started a campaign to reduce them. Our survey resulted in finding new values of the rotation period for a quarter of the studied sample of long-period and low-amplitude asteroids. Majority of the revised periods occurred to be longer than it seemed previously. The diameters of our current targets are mostly large, around a few tens of kilometers. Since the timescale of YORP effectiveness is proportional to the radius squared (Rubincam, 2000), in the size range studied here this effect is probably negligible. Also, the damping timescales for tumbling asteroids in this size range are a fraction of the age of the Solar System (Pravec et al., 2005). So the low rotation frequencies found here are most probably primordial, or can in part be an outcome of major collisions in the epoch when the Main Belt was much more populated. Basing on these facts we expect mostly prograde rotations of these asteroids, as an outcome of growth from small pebbles embedded in the protoplanetary gas disc (Johansen and Lacerda, 2010), and no substantial trends for spin axis positions. Low frequency also implies that the internal structure can be more loosely bound than if the frequency was higher. Consequently, the expected bulk densities in this class of objects can be lower, implying larger macroporosity. The shapes of these objects have low probability of being rotationally reshaped or disrupted. Their asymmetric lightcurves imply irregular shapes.

Our findings strengthen the need to study such targets, even though they are observationally demanding. We are planning to observe these, and also fainter (smaller) targets in future apparitions, until the data suffice for obtaining unique spin and shape models. The improved statistics of periods, spins, and shapes will allow making more robust conclusions on the present state and previous history of the Solar System with both violent collisions and subtle thermal forces influencing those minor bodies.

## Acknowledgements

This work was partially supported by Grant no. 2014/13/D/ST9/01818, D.O. was supported by Grant no. 2012/04/S/ST9/00022, K.K. by Grant no. UMO-2011/01/D/ST9/00427, and M.P. by Grant no. 2014/13/B/ST9/00902 all from the National Science Centre, Poland. The work of T.S.R. was carried out through the Gaia Research for European Astronomy Training (GREAT-ITN) network. He received funding from the European Union Seventh Framework Programme (FP7/2007–2013) under Grant agreement no. 264895.

The Joan Oró Telescope (TJO) of the Montsec Astronomical Observatory (OAdM) is owned by the Catalan Government and operated by the Institute for Space Studies of Catalonia (IEEC).

Data from Pic du Midi Observatory have been obtained with the 0.6 m telescope, a facility operated by observatoire Midi-Pyrénées and Association T60, an amateur association. We thank N. Takahashi, and the staff members of Bisei Spaceguard Center for their support. We also acknowledge the Japan Space Forum.

## Appendix A

Period spectra for targets with revised periods are shown in Figs. A1–A8.

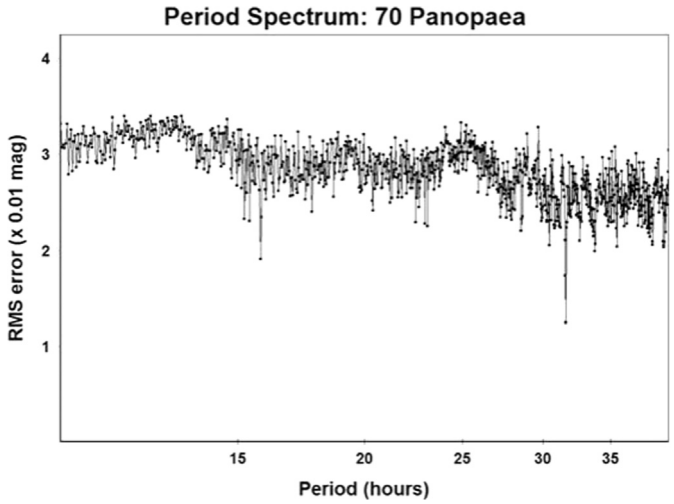


**Fig. A1.** Period spectrum for (70) Panopaea based on data from the year 2014. Lowest rms for $P=31.619$ h.

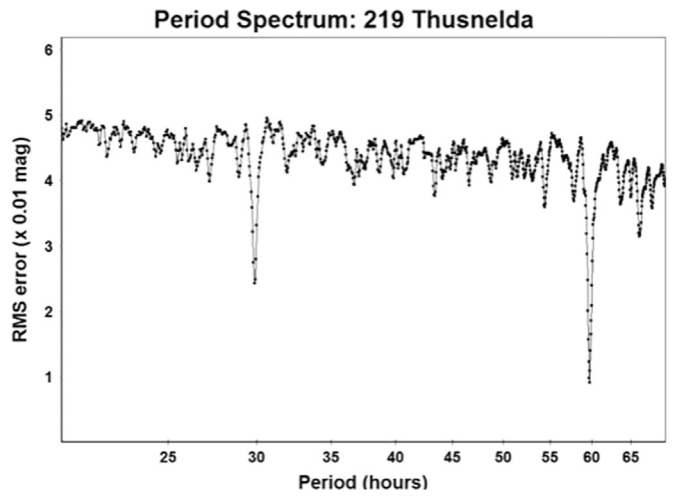


**Fig. A2.** Period spectrum for (219) Thusnelda based on data from the year 2014. Lowest rms for $P=59.74$ h.

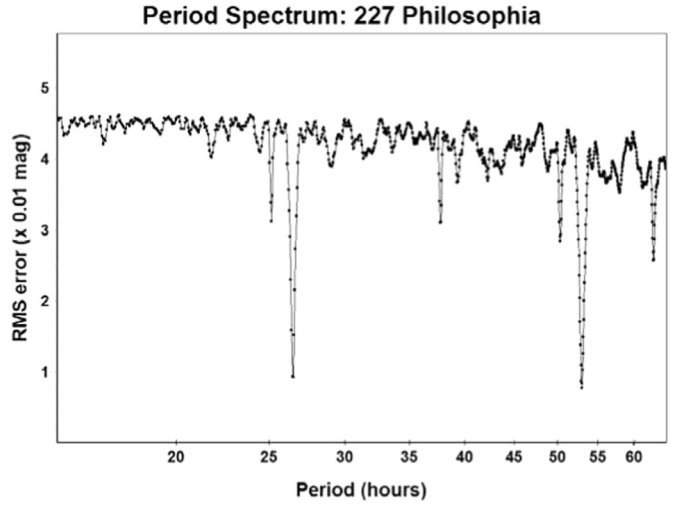


**Fig. A3.** Period spectrum for (227) Philosophia based on data from the years 2013/2014. Accepted period $P=26.46$ h.

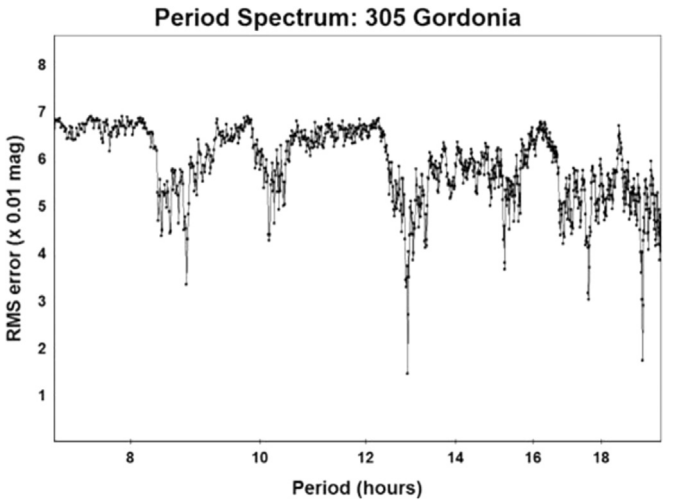


**Fig. A4.** Period spectrum for (305) Gordonia based on data from the year 2014. Lowest rms for $P=12.893$ h.

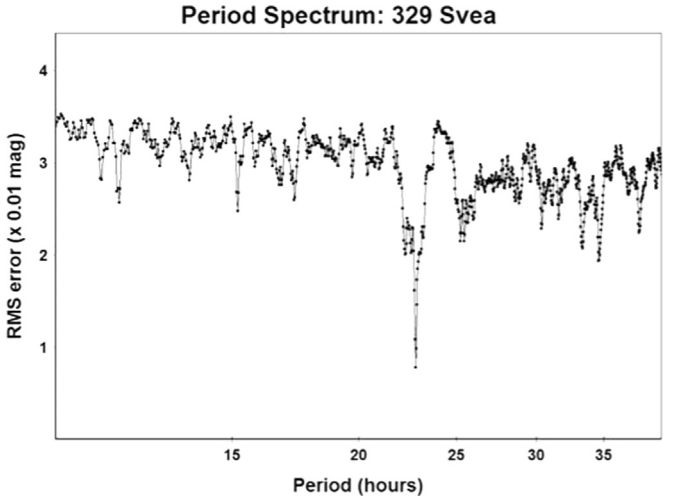


**Fig. A5.** Period spectrum for (329) Svea based on data from the year 2013. Lowest rms for $P=22.778$ h.

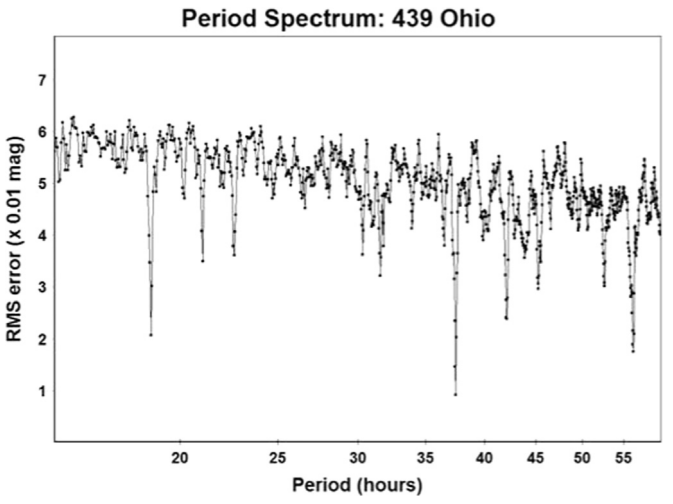


**Fig. A6.** Period spectrum for (439) Ohio based on data from the year 2014. Lowest rms for $P=37.46$ h.

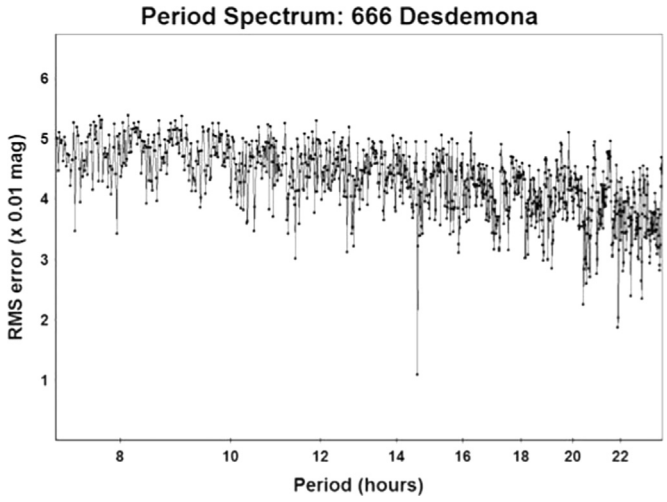


**Fig. A7.** Period spectrum for (666) Desdemona based on data from the years 2013/2014. Lowest rms for $P=14.607$ h.

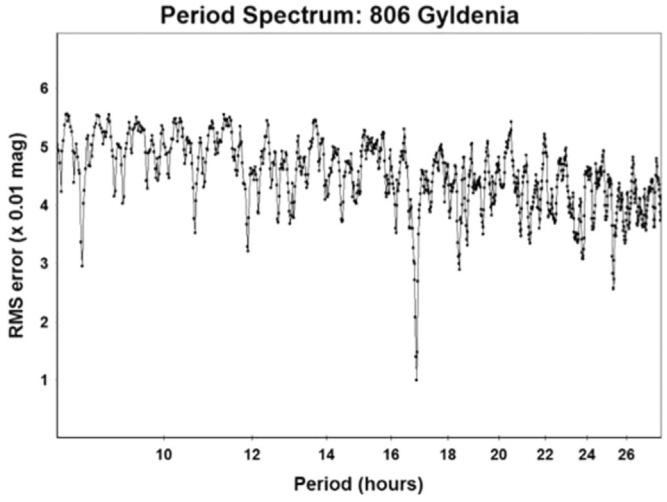


**Fig. A8.** Period spectrum for (806) Gyldenia based on data from the year 2013. Lowest rms for $P=16.852$ h.

## References


Alkema, M.S., 2013a. Minor Planet Bull. 40, 133.
Alkema, M.S., 2013b. Minor Planet Bull. 40, 215.
Behrend, R., et al., 2014. Observatoire de Geneve Web Site. ⟨http://obswww.unige.ch/~behrend/page_cou.html⟩ (state for 15 December).
Bembrick, C.S., Allen, B., Richards, T., 2006. Minor Planet Bull. 33, 42.
Bowell, E., Oszkiewicz, D.A., Wasserman, L.H., et al., 2014. Meteoritics Planet. Sci. 49, 95.
Denchev, P., Magnusson, P., Donchev, Z., 1998. Planet. Space Sci. 46, 673.
Ditteon, R., Hawkins, S., 2007. Minor Planet Bull. 34, 59.
Harris, A.W., Young, J.W., 1989. Icarus 81, 314.
Harris, A.W., Young, J.W., Dockweiler, T., Gibson, J., et al., 1992. Icarus 95, 115.
Harris, A.W., Pravec, P., Galád, A., et al., 2014. Icarus 235, 55.
Hanuš, J., Ďurech, J., Brož, M., et al., 2011. Astron. Astrophys. 530, A134.
Hanuš, J., Ďurech, J., Brož, M., et al., 2013. Astron. Astrophys. 551, A67.
Jedicke, R., Metcalfe, T.S., 1998. Icarus 131, 245.
Johansen, A., Lacerda, P., 2010. Mon. Not. R. Astron. Soc. 404, 475.
Kryszczyńska, A., 2013. Astron. Astrophys. 551, A102.
Lagerkvist, C.-I., Kamel, L., 1982. Moon Planets 27, 463.
Lagerkvist, C.-I., Hahn, G., Magnusson, P., Rickman, H., 1987. Astron. Astrophys. Suppl. Ser. 70, 21.
Lazar, S., Lazar, P., Cooney, W., Wefel, K., 2001. Minor Planet Bull. 28, 32.
La Spina, A., Paolicchi, P., Kryszczyńska, A., Pravec, P., 2004. Nature 428, 400.
Magnusson, P., Lagerkvist, C.-I., 1990. Astron. Astrophys. 86, 45.
Marciniak, A., Michałowski, T., 2010. Astron. Astrophys. 512, A56.
Marciniak, A., Bartczak, P., Santana-Ros, T., et al., 2012. Astron. Astrophys. 545, A131.
Menke, J., Cooney, W., Gross, J., Terrell, D., 2008. Minor Planet Bull. 35, 155.
Michałowski, T., Kwiatkowski, T., Kaasalainen, M., et al., 2004. Astron. Astrophys. 416, 353.
Pilcher, F., Alkema, M.S., 2014a. Minor Planet Bull. 41, 188.
Pilcher, F., Alkema, M.S., 2014b. Minor Planet Bull. 41, 233.
Pravec, P., Harris, A.W., Scheirich, P., 2005. Icarus 137, 108.
Pravec, P., Harris, A.W., 2000. Icarus 148, 12.
Pravec, P., Harris, A.W., 2007. Icarus 190, 250 ⟨http://www.asu.cas.cz/~asteroid/binastdata.htm⟩ (updated September 25, 2013).
Pray, D.P., 2006. Minor Planet Bull. 33, 4.
Rubincam, D.P., 2000. Icarus 148, 2.
Santana-Ros, T., Bartczak, P., Michałowski, T., Tanga, P., Cellino, A., 2015. Mont. Not. R. Astron. Soc. 450, 333.
Schroll, A., Schober, H.J., 1983. Astron. Astrophys. Suppl. Ser. 53, 77.
Stephens, R.D., 2001. Minor Planet Bull. 28, 28.
Warner, B.D., Harris, A.W., Pravec, P., 2009. Icarus 202, 134 ⟨http://www.MinorPlanet.info/lightcurvedatabase.html⟩ (updated November 10, 2012).
Weidenschilling, S.J., Chapman, C.R., Davis, D.R., Greenberg, R., et al., 1990. Icarus 86, 402.